Article:
Ai, Q, Ding, B, Liu, Q et al. (2016) A subject-specific EMG-driven musculoskeletal model for applications in lower-limb rehabilitation robotics. International Journal of Humanoid Robotics, 13 (03). 1650005. ISSN: 0219-8436

https://doi.org/10.1142/S0219843616500055

A SUBJECT-SPECIFIC EMG-DRIVEN MUSCULOSKELETAL MODEL FOR APPLICATIONS IN LOWER-LIMB REHABILITATION ROBOTICS

QINGSONG AI[†], BO DING[‡], QUAN LIU[§], WEI MENG[ξ]

Key Laboratory of Fiber Optic Sensing Technology and Information Processing, Ministry of Education, School of Information Engineering, Wuhan University of Technology, 122 Luoshi Road, Wuhan, 430070, China

[†]*qingsongai@whut.edu.cn*

[‡]*whut_db@163.com*

[§]*liuquanwhut@163.com*

[ξ]*weimeng@whut.edu.cn*

Received Day Month Year
Revised Day Month Year
Accepted Day Month Year

Robotic devices have great potential in physical therapy owing to their repeatability, reliability and cost economy. However, there are great challenges to realize active control strategy, since the operator's motion intention is uneasy to be recognized by robotics online. The purpose of this paper is to propose a subject-specific electromyography (EMG)-driven musculoskeletal model to estimate subject's joint torque in real time, which can be used to detect his/her motion intention by forward dynamics, and then to explore its potential applications in rehabilitation robotics control. The musculoskeletal model uses muscle activation dynamics to extract muscle activation from raw EMG signals, a Hill-type muscle-tendon model to calculate muscle contraction force, and a proposed subject-specific musculoskeletal geometry model to calculate muscular moment arm. The parameters of muscle activation dynamics and muscle-tendon model are identified by off-line optimization methods in order to minimize the differences between the estimated muscular torques and the reference torques. Validation experiments were conducted on six healthy subjects to evaluate the proposed model. Experimental results demonstrated the model's ability to predict knee joint torque in high- accuracy with the coefficient of determination (R^2) value of 0.934 ± 0.013 and the normalized root-mean-square error (RMSE) of $11.58\% \pm 1.44\%$.

Keywords: EMG signals; musculoskeletal modeling; rehabilitation robotics; control strategies.

1. Introduction

Elderly people are vulnerable to neurologic impairments such as stroke and paralysis. Many of these survivals suffer from motor impairments that seriously affect their daily lives. In recent years, there is an increasing interest in developing robotics for rehabilitation and various robot control strategies have been proposed.[1, 2] Robotics can relieve the therapists from the heavy rehabilitation task and facilitate repetitive, systematic and prolonged rehabilitation training.[3] Despite the advantages of assistive robotics in rehabilitation, it is difficult to realize human-active control strategy on robotics. On one hand, to realize the robot-aided rehabilitation training, a human-robot interface must be established to help the robot understand the motion intention of the

operator.[4] On the other hand, the robotic assistance should be adjustable to meet the needs of patients in different rehabilitation stages.

EMG signals have been widely used in human-robot interface design since they are the direct measures of muscle's electrical activity. Recently, several well-developed methods using EMG signals to distinguish the operator's different motion patterns have been proposed.[5-7] Robot control performance by using this kind of method largely depends on the classification accuracy. The main drawback of this method relates to two separated movements, an active patient-triggered phase and a passive robot-driven phase.[8] As a result, the patient only applies voluntary efforts in the first phase and has no interaction in the second phase. In this situation, the rehabilitation course is actually charged by the robot. On the other hand, a continuous motion must be divided into some discrete motion patterns. To make the discrete motions more approximate to the original ones, the number of patterns must be increased. However, the increase of patterns will lead to the decrease of classification accuracy and make the classification algorithm more complex.[9]

To overcome these shortcomings, recent researches have worked toward using EMG signals to estimate joint torque applied by the operator. This torque estimation based method aims at providing operators with continuous assistance. Generally speaking, there are two approaches that can be used to transform the EMG signals into joint torque: black-box and musculoskeletal model. A black-box method using recurrent artificial neural network to estimate torque of elbow was proposed by Song et al.[10] Kiguchi et al. designed an exoskeletal robot to assist elbow motion and a fuzzy neuro algorithm was applied to establish the relation between EMG signals and elbow joint torque.[11] The main advantage of black-box method is that the complex and nonlinear relationship between EMG signals and joint torque can be avoided and only input and output training samples are required.

However, this kind of method can not provide insight into the biomechanical process of human movement. A possible solution to this problem is to estimate the torque applied by operators based on musculoskeletal model. A systematic review on model based muscle force and joint torque estimation methods was presented by Erdemir et al.[12]. Moreover, a musculoskeletal model based assist-as-needed (AAN) control method was proposed by Carmichael,[13, 14] where a musculoskeletal model was developed to calculate the operator's strength with respect to different tasks. However, their model was not specific to the subjects' different muscle-tendon properties. A generic model (model parameters were collected from published data) was employed to analysis the strength of all subjects. Since they primarily focused on the assistance needed to perform different tasks, using the generic model to estimate strength is suitable. But if quantitative analysis is need for each patient's physical capability, the generic model will be inappropriate. To this end, an off-line parameter identification procedure was performed to adjust the musculoskeletal model to match specific subjects.[15] Similarly, a musculoskeletal model to study movements of elbow joint was developed by Pau et al.[16] In their studies, only EMG signals collected from the involved muscles were used to predict elbow motions.

Therefore, the additional data processing steps with respect to other information such as joint kinematics can be omitted.

Knee is the largest and most complicated joint in human body, which plays an important role in human motions. Currently, there are few musculoskeletal models for knee joint have been developed. Moreover, some researchers did not study the subject-specific musculoskeletal geometry, which is vital to calculate muscle contraction force and to understand each muscle's contribution to total muscular torque. To match specific subjects, the geometry path can be scaled based on relative distances between pairs of markers obtained from a motion-capture system. However, the motion-capture system is quite expensive. Furthermore, the applications of these models were limited to clinical diagnosis and management of orthopaedic conditions.[12, 16] Hence, their potential applications in robot control and rehabilitation need to be further investigated.

In this paper, a subject-specific musculoskeletal model for knee joint is presented to estimate the subject's joint torque, which can greatly reflect the subject's motion intention. In order to adjust the musculoskeletal model parameters to specific subjects, off-line identification processes are carried out. Furthermore, the model is re-calibrated to investigate whether the proposed model with subject-specific musculoskeletal model can improve prediction accuracy compared to models with generic musculoskeletal geometry. After this, preliminary experiments are conducted to explore its potential applications in robot active control. Finally, a detailed discussion of benefits and limitations of the proposed model and model based control approach is also presented and compared with the existing methods.

2. Methods

Musculoskeletal model can be used to elucidate the biomechanical process of human motion which begins with the neural command and ends with the joint kinematics. Generally, the model can be divided into three parts, namely, muscle activation dynamics, Hill-type muscle-tendon model and musculoskeletal geometry.[17, 18] In this work, the musculoskeletal model in relation to knee joint is taken into account. The model includes eight muscles which were supposed to be main actuators for knee joint rotation. Muscles that contribute to knee extension are Rectus Femoris (RF), Vastus Lateralis (VL), Vastus Medialis (VM) and Vastus Intermedius (VI). In addition, Biceps Femoris long/short head (BFL, BFS), Semimembranous (SM) and Semitendinosus (ST) are four knee flexors.[19]

2.1. *EMG pre-process and muscle activation dynamics*

Muscle activation, represented by $a(t)$, implies the amount of force that the neural system requires the muscle to generate. Extracting muscle activation from raw EMG signals is necessary for estimating muscle contraction force. The raw EMG signals were pre-processed by a high-pass filter with a 25Hz cut off frequency, and then were rectified and normalized. After the normalization was done, the resultant signals were low-pass

filtered (cut off frequency 3 Hz) to simulate the muscle's natural property that acts as a low-pass filter. The processed EMG signals are expressed by $e(t)$, which was input to a model to obtain the neural activation $u(t)$, as expressed in Eq.(1) , where d is the electromechanical delay and γ, β_1 and β_2 are proportional coefficients. In order to make the equation stable and limit its solution (0 to 1), the constrains as shown in Eq.(2) must be met. After $u(t)$ was determined, a simple solution[20] can be used to calculate the muscle activation by using Eq.(3), where A is the nonlinear shape factor that varies from -3, when the relationship is highly exponential, to 0, when the relationship is linear.

$$u(t) = \gamma e(t-d) - \beta_1 u(t-1) - \beta_2 u(t-2) \tag{1}$$

$$\beta_1 = c_1 + c_2,\ \beta_2 = c_1 \cdot c_2,\ \gamma - \beta_1 - \beta_2 = 1.0 \text{ and } |c_1| < 1, |c_2| < 1 \tag{2}$$

$$a(t) = \frac{e^{Au(t)} - 1}{e^{A} - 1} \tag{3}$$

2.2. *Hill-type muscle-tendon model*

This section explains how to calculate the muscle force by using Hill-type muscle-tendon model. The relationship between the length of muscle-tendon L_{mt}, the muscle fiber length L_m and tendon length L_t can be described by Eq.(4), where α is the pennation angle. Muscle-tendon force F can be obtained according to Eq.(5), where F_t is the tendon force, F_m the muscle fiber force, $F_m^{\max}$ the maximum isometric muscle force, $\tilde{L}_m$ the normalized muscle fiber with respect to the optimal muscle fiber length L_m^o , $\tilde{V}_m$ the normalized muscle fiber contraction velocity with respect to maximal muscle contraction velocity $V_{\max}$ and a the muscle activation explained above. $\tilde{F}_A(\tilde{l}_m)$, $\tilde{F}_V(\tilde{v}_m)$ and $\tilde{F}_P(\tilde{l}_m)$ are the normalized active force-length, force-velocity and passive force-length function, respectively.[21]

$$L_{mt} = L_m \cos\alpha + L_t \tag{4}$$

$$F = F_m^{\max}[\tilde{F}_A(\tilde{L}_m) \cdot \tilde{F}_V(\tilde{V}_m) \cdot a + \tilde{F}_P(\tilde{L}_m)]\cos\alpha \tag{5}$$

Once the muscle fiber length L_m and its contraction velocity V_m are determined, the muscle force can be calculated by using Eq.(5). However, it is difficult to obtain L_m directly, since it can only be measured by medical devices such as magnetic resonance imaging (MRI) systems or ultrasonic scanner, which are not available in laboratory environment. Actually, L_m can be indirectly obtained by Eq.(4), and L_{mt} can be estimated by the muscle path and knee joint kinematics, which will be discussed in the next section. Moreover, L_t can be computed by the normalized tendon-force relationship $\tilde{F}_t(L_t)$ presented as in Eq.(6), where ε is the optimal tendon strain and L_t^s is the tendon slack length. Finally, the muscle-tendon force can be estimated according to Eq.(7).[22] A block diagram (Fig. 1) was provided to make the calculation process more explicit.

$$\tilde{F}_t(L_t) = \begin{cases} \dfrac{0.33}{e^3 - 1}\left(e^{\frac{3}{0.069\varepsilon} \bullet \frac{(L_t - L_t^s)}{L_t^s}} - 1\right), & L_t \le 0.609\varepsilon \bullet L_t^s + L_t^s \\ \dfrac{1.712}{\varepsilon}\left(\dfrac{(L_t - L_t^s)}{L_t^s} - 0.609\varepsilon\right) + 0.33, & else \end{cases} \tag{6}$$

$$F = F_t = F_m \cos\alpha \tag{7}$$

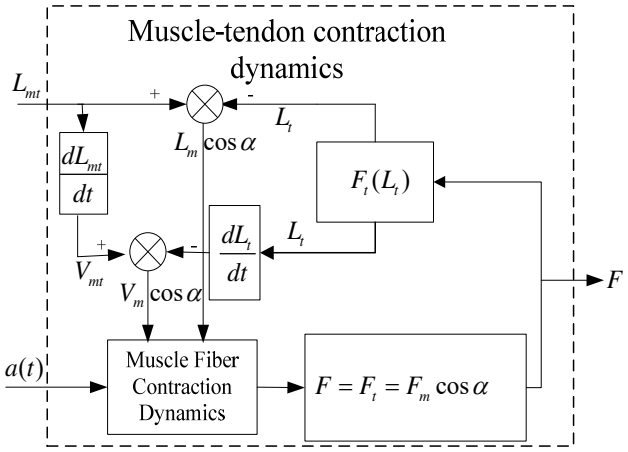

Fig.1. Block diagram of muscle-tendon contraction dynamics

2.3. *Subject-specific musculoskeletal geometry model*

Moment is the product of force and its moment arm. To compute a muscle-tendon moment arm, muscle paths are required to determine the muscle's length and its line of action. Generally, muscle paths can be determined by the aforementioned medical devices. However, the use of medical devices is expensive and time-consuming.[23] It is therefore many researchers employed a generic musculoskeletal geometry model established with reported data collected from cadavers to calculate muscle-tendon length and moment arm. However, the generic musculoskeletal geometry may not suitable for specific individuals and subject-specific musculoskeletal geometry is essential for the improvement of moment prediction accuracy. To match the specific subject, the geometry path can be scaled based on relative distances between pairs of markers obtained from a motion-capture system. However, the motion-capture system is quite expensive. A practical solution is proposed here to tackle this problem. For simplicity, the muscles are assumed as straight lines.[17] Since the muscle path can be affected by the size of bones, the length of body segment and attachment sites, muscles' origin coordinates and insertion coordinates are estimated based on the skeletal morphologic parameters

measured from lower extremity and the related regress equations.[24] A typical subject's muscle paths in the standard standing pose can be found in Table 1.

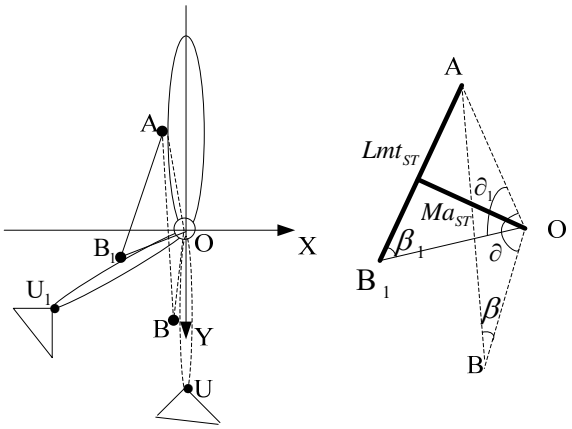

Fig.2. Illustration of musculoskeletal geometry model

Once the static muscle paths are determined, the subject-specific musculoskeletal geometry model can be established and the dynamic muscle-tendon moment arm can be obtained. Without loss of generality, the calculation of just ST's moment arm is described. As shown in Fig.2, the dash line represents the static standing pose and the solid line indicates the dynamic pose. A is the origin point, B is the insertion point and O is the center of knee joint. Hence, the muscle-tendon length and moment arm can be determined by the following equations.

$$Lmt_{ST} = \sqrt{l_{AO}^2 + l_{B_1O}^2 - 2l_{AO}l_{B_1O}\cos\partial_1} \tag{8}$$

$$Ma_{ST} = l_{BO}\sin\beta_1 \tag{9}.$$

Table 1 The muscle paths of a typical subject

Muscle	Origin Coordinates(cm)			Coordinate	Insertion Coordinates(cm)			Coordinate
	x	y	z	System	x	y	z	System
BFS	1.196	11.825	2.134	femur	0.183	33.570	5.417	tibia
BFL	-5.103	-4.810	1.826	pelvis	0.183	33.570	5.417	tibia
ST	-5.103	-4.810	1.826	pelvis	-0.390	32.858	-1.848	tibia
SM	-5.021	-4.741	0.895	pelvis	-0.390	32.858	-1.848	tibia
RF	4.218	3.501	2.047	pelvis	3.905	2.435	-0.767	femur
VL	1.584	18.723	3.435	femur	3.905	2.435	-0.767	femur

VM	0.210	17.009	1.427	femur	3.905	2.435	-0.767	femur
VI	2.782	27.898	2.762	femur	3.905	2.435	-0.767	femur

3. Model identification and validation

3.1 Parameter identification

In order to make muscle-tendon model parameters match specific subjects, identification experiments should be carried out. As aforementioned, d , c_1 , c_2 and A are four parameters used to define the muscle activation dynamics. It is assumed that all involved muscles share the common activation dynamics. Hence, only 4 activation parameters need to adjust. As to the muscle-tendon model, $F_m^{\max}$, L_m^o , L_t^s , $V_{\max}$ and α are five anatomical parameters that reflect the force-generating ability of each muscle. Among these muscle parameters, $F_m^{\max}$, L_m^o and L_t^s have shown high sensitivities[25, 26] and $V_{\max}$ can be set to $10L_m^o$. Thus only three parameters need to be identified for each muscle-tendon model. Since 8 muscles were taken into consideration, a total of 24 muscle-tendon model parameters should be identified by optimization methods. Combining forward and inverse dynamics, these parameters can be tuned based on the principle that the net joint moment estimated by the EMG-driven forward dynamics model are supposed to be in accordance with moment obtained by inverse dynamics,[18] as given by Eq.(10) and Eq.(11), where M_{net} is the net knee joint moment, $M_{mus} = \sum ma_i \times F_i$ is the joint moment generated by muscles, M_{gra} the gravitational moment of the lower limb, M_{pass} the passive joint moment.

$$M_{net} = M_{mus} - M_{pass} - M_{gra} \tag{10}$$

$$M_{net} = J \bullet \ddot{\theta}_k \tag{11}$$

Note that it is difficult to model the passive joint moment due to the complexity of joint components and construct. In addition, it is found that most values of the passive joint moment were small when the joint angles were within a certain range (e.g. $-50^\circ < \theta_k < 80^\circ$). And when the joint angles were close to the joint limits, the passive joint moment would rise sharply.[27] In terms of rehabilitation training, the range of movement (ROM) is always moderate, thus, M_{pass} was neglected for simplicity, and then the net joint M_{net} can be determined by M_{mus} and M_{gra} . Furthermore, M_{net} can also be calculated by Eq.(11), where J is the moment of inertial of the lower limb and $\ddot{\theta}_k$ is the angular acceleration obtained by differentiating the angular position twice. Finally, the principle of parameter identification process can be simplified as shown in Eq.(12).

$$M_{mus} = M_{gra} + J \bullet \ddot{\theta}_k \tag{12}$$

3.2. Model validation

The goal of the model validation procedure is two fold: 1) to evaluate the feasibility and effectiveness of the proposed EMG-driven musculoskeletal model. 2) to test whether the proposed model with subject-specific musculoskeletal geometry can improve the prediction accuracy compared to models with generic musculoskeletal geometry.

The validation experiments were conducted on six healthy subjects. In the experiment, without taking into account the effects of ground reaction force (GRF), each subject was asked to sit on a chair with his/her feet being off the ground. After the maximal EMG signals were collected during the maximum voluntary contraction (MVC) experiments, the subjects were asked to perform extension and flexion movements of knee joint at arbitrary speed. Note that when the subject was in a sitting position, the knee angle θ_k was limited to vary from about -60 to 90 degree, where the negative values indicate the knee flexion. Specially, θ_k will be 0 when the subject is at rest. During the experiment, raw EMG signals were recorded by the EMG acquisition equipment (DataLOG MWX8, Biometrics Ltd. UK) and sampled at the rate of 1000 Hz. It is assumed that the activations of SM and BFS are equal to ST and BFL, respectively and the activation of VI can be calculated using the activations of VL and VM.[20] For each subject, only five muscles (RF, VL, VM, BFL, ST) were thus taken into consideration (The EMG electrodes placements can be found in Fig.6). At the meantime, angular position of knee joint was recorded by a wearable angular transducer. The subjects were asked to have enough rest after each trial to eliminate the effects of muscle fatigue.

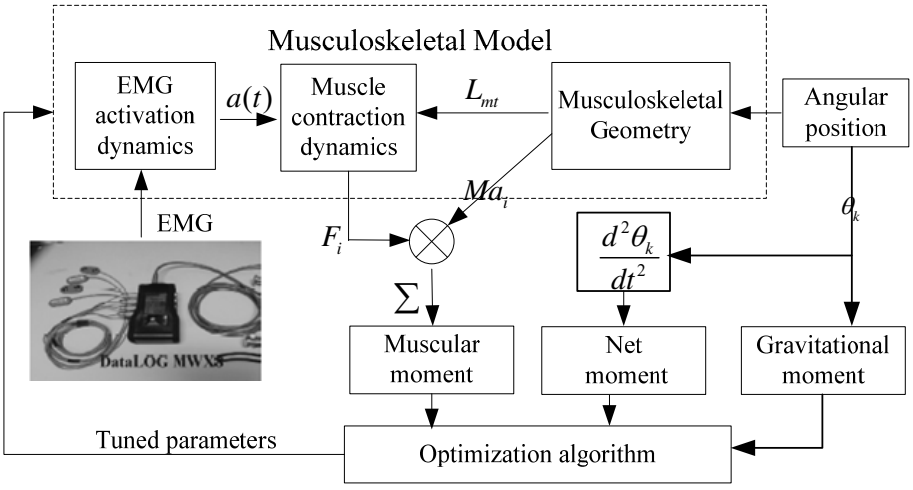

Fig.3. Block diagram of parameters identification process

Two groups of optimization process were performed to achieve the goals of the validation procedure. In the first group G1, the muscular moment was estimated by the proposed model with the subject-specific musculoskeletal geometry. In the second group G2, the subject-specific musculoskeletal geometry was replaced by a generic model. For

each group, both raw EMG signals and kinematics data were input to the optimization model as shown in Fig.3 to identify the parameters of musculoskeletal model. In order to make the resultant parameters physiologically meaningful and improve the optimization performance, the initial values of model parameters were obtained from the reported data and were allowed to vary within the limited ranges. In this study, the off-line optimization process was done by using MATLAB Simulink. And a nonlinear least square method with the Levenberg Marquardt algorithm was adopted to adjust the parameters during the identification process to minimize the differences between the estimated moment and the reference moment.

3.3. Results

Without loss of generality, typical results of two subjects (S4 and S6) were selected to elucidate the process. The raw EMG signals measured from lower limb are illustrated in Fig.4. Comparisons between the estimated muscular torque and the reference torque are shown in Fig.5. Furthermore, a summary of estimation performance of the model of all subjects is presented in Table 2 and the tuned model parameters for all six subjects are presented in Table 3.

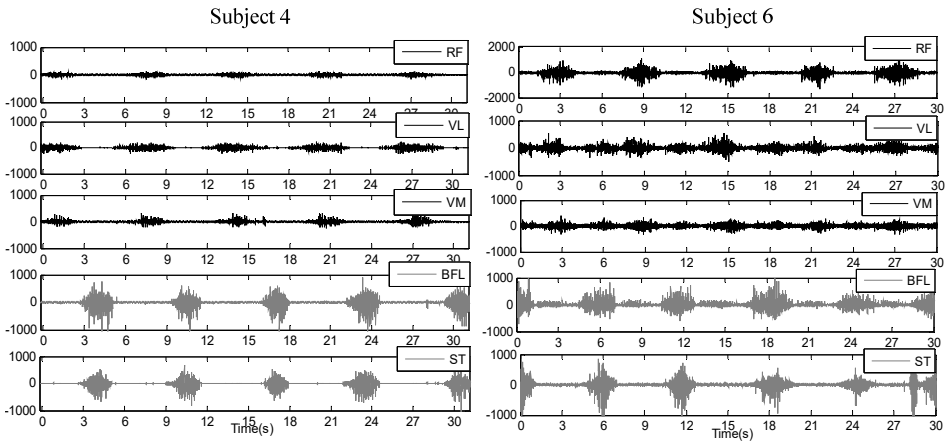

Fig.4. Raw EMG signals. The black line indicates the EMG signals measured from extensors and the gray line represents the EMG signals obtained from flexors.

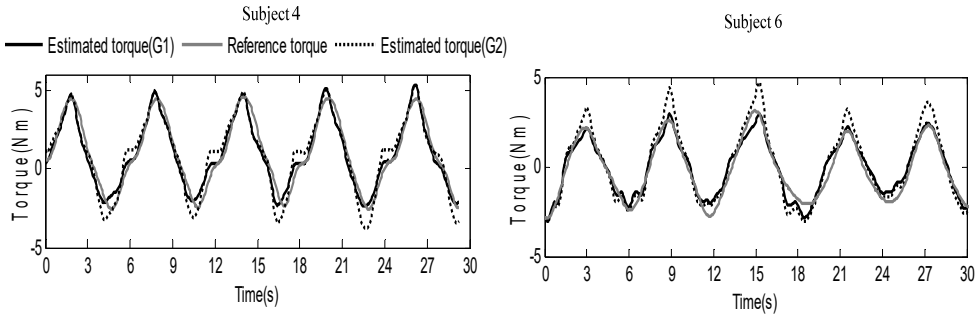

Fig.5. Comparison of torque (+, knee extension; -, knee flexion). The black solid line is the estimated muscular torque in the first group G1 and the black dashed line represents the estimated torque in the second group G2. The gray line indicates the reference torque calculated by Eq.(12).

Fig.4 clearly shows that the muscle activation pattern varies from subject to subject. For example, the EMG values of RF measured from subject 4 were notably smaller that that collected from subject 6. However, for each subject when performing knee extension movements the main actuators are the same, namely, RF, VL, VI and VM. Conversely, the knee flexion is attributed to contractions of BFL, BFS, ST and SM, and the EMG signals measured from quadriceps femoris are negligible during this movement. One can see that the EMG signals obtained from extensors/flexors are always changing simultaneously, although they are different in amplitude. This co-activation of different muscles can be termed as muscle synergy, which was suggested as an efficient way to facilitate complex movements.[28] Combining with Fig.5, one can note that the estimated muscular torque increased with the EMG values. The main reason for this is that the active muscle force is proportional to muscle activation according to Eq.(5). As mentioned earlier, the subject could freely perform knee extension/flexion movements and the GRF was ignored, consequently the estimated muscular torque is approximate to the gravitational torque which changed sinusoidally during the experiments.

Table 2 Summary of prediction performance of the model

Subject	Group	Coefficient of determination(R^2)	Maximum moment deviation ΔM (Nm)	Normalized RMSE (Nm)
S1	G1	0.935	1.50	10.68%
	G2	0.905	1.62	14.46%
S2	G1	0.923	1.40	11.20%
	G2	0.911	1.42	12.60%
S3	G1	0.949	1.20	10.78%
	G2	0.925	2.09	13.35%
S4	G1	0.946	1.06	10.49%
	G2	0.886	2.24	16.46%
S5	G1	0.936	1.31	12.03%

	G2	0.893	2.06	17.38%
S6	G1	0.916	1.03	14.30%
	G2	0.884	1.82	19.20%
Mean	G1	0.934	1.250	11.58%
	G2	0.900	1.875	15.57%
SD	G1	0.013	0.187	1.44%
	G2	0.016	0.313	2.54%

(*Note*: Normalized RMSE $= \frac{\text{RMSE}}{\text{Peak Moment}}$, SD=Standard Deviation)

Fig.5 illustrates the ability of the proposed EMG-driven musculoskeletal model to predict knee joint torque for two subjects when performing extension/flexion movements. Despite the differences between subjects such as muscle activation patterns, the proposed model can be tuned to track the knee joint torque with an acceptable accuracy. Both the shape and magnitude (the green dashed line) of the estimated torque are in good agreement with the reference torque. A high level of correlation (the R^2 value ranging from 0.916 to 0.949) and a low normalized RMSE (from 10.49% to 14.30%) were obtained as presented in Table 2, which demonstrates the feasibility and effectiveness of the proposed model.

Table 3 The tuned and published musculoskeletal model parameters

Muscle/Subject $F_m^{\max}$ (N) L_t^s (m) L_m^o (m)	S1	S2	S3	S4	S5	S6	Delp
	789	688	800	793	815	821	780
RF	0.286	0.297	0.275	0.268	0.273	0.283	0.346
	0.076	0.082	0.084	0.083	0.084	0.095	0.084
	259	400	272	141	156	384	431
BFS	0.077	0.127	0.056	0.091	0.089	0.119	0.100
	0.175	0.181	0.175	0.171	0.168	0.186	0.173
	798	696	727	704	754	657	1870
VL	0.146	0.208	0.176	0.120	0.1655	0.192	0.157
	0.08	0.101	0.082	0.072	0.083	0.094	0.082
	339	343	251	281	242	388	720
BFL	0.279	0.313	0.268	0.268	0.273	0.306	0.341
	0.113	0.124	0.086	0.099	0.099	0.114	0.109

	1095	687	1299	611	1100	758	1295
VM	0.094	0.110	0.146	0.108	0.137	0.104	0.126
	0.072	0.129	0.05	0.072	0.069	0.101	0.089
	139	182	133	146	111	282	330
ST	0.259	0.287	0.263	0.260	0.257	0.249	0.262
	0.225	0.249	0.198	0.201	0.205	0.210	0.201
	502	364	800	414	525	321	1235
VI	0.145	0.165	0.155	0.116	0.137	0.155	0.136
	0.075	0.104	0.051	0.077	0.087	0.117	0.087
	420	564	349	356	344	303	1030
SM	0.256	0.308	0.257	0.325	0.262	0.311	0.359
	0.080	0.113	0.082	0.078	0.092	0.109	0.080

As mentioned before, the model was re-calibrated with a generic musculoskeletal geometry in the second group G2. It is evident that there were differences between the estimated muscular torques in the two groups and the estimated torque in G1 is in better agreement with the reference torque compared with that in G2. In addition, the predicted joint torque R^2 reduced from 0.934 to 0.900 and the normalized RMSE values increased from 11.58% to 15.57%, as shown in Table 2. More specifically, in G1 the R^2 values are higher, the normalized RMSEs and maximum moment deviations are smaller across all subjects compared with that in G2, indicating the proposed model is capable of providing better representations of the subjects involved in this study.

Table 3 clearly shows that the identified parameters are different with the published data.[29] It demonstrates that the muscle-tendon model parameters have large individual-to-individual variation. When the reported data were directly used to compute joint torque, poor prediction performance was observed (R^2 =0.21 and normalized RMSE=142%). Hence, it is imperative to identify the subject-specific parameters to make the estimation more accurate.

4. Model Applications

4.1. Preliminary experiments with a lower-limb rehabilitation robot

The objective of the experiments in this section include: 1) to test whether the musculoskeletal model can predict the operator's motion intention in real time. 2) to explore its potential applications in rehabilitation robot control. In this study, preliminary experiments were conducted on one of the six subjects with a parallel robot system developed by our research group. The robot system mainly consists of a robot platform, a DSP controller cabinet and a PC. The robot platform has six degrees of freedom (DOFs),

namely, three transitional DOFs and three rotational DOFs. The detailed description of the robot system is available in our previous work.[30, 31]

(a) (b)

Fig.6. (a) The parallel robot system; (b) EMG electrodes placements for the involved 5 muscles

In order to realize human-active robot control, the control interface should be capable of detecting the participant's motion intention and be adjustable to meet the requirements of different operators. The operator's muscular moment here can be estimated by the proposed EMG-driven model, his/her motion intention can be detected based on forward dynamics. Firstly, the angular acceleration can be given by Eq.(13), where λ is a parameter which was intentionally introduced to represent the level of assistance. Then the new angular velocity and angular position can be obtained by Eq.(14) and Eq.(15), where $\dot{\theta}_i$ and θ_i are the previous angular velocity and angular position at time step *i*, respectively. Similarly, $\dot{\theta}_{i+1}$ and θ_{i+1} are new angular velocity and angular position at the next time step *i+1*, respectively, and τ is the sampling period.

$$J \bullet \ddot{\theta} = (1+\lambda) M_{mus} - M_{gra} \tag{13}$$

$$\dot{\theta}_{i+1} = \dot{\theta}_i + \ddot{\theta} \bullet \tau \tag{14}$$

$$\theta_{i+1} = \theta_i + \dot{\theta}_i \bullet \tau + \frac{\ddot{\theta}}{2} \bullet \tau^2 \tag{15}$$

Three control modes were designed in the first group of experiments to explore applications of the proposed model. In mode *a*, the parameter λ was set to 0 (free mode is simulated), which aimed to investigate whether the model based control interface can accurately detect the subject's motion intention in real time. In this situation, the robot was controlled to track the subject's movement trajectory. In mode *b*, λ was set to 0.5 (assistive mode is simulated), which meant the operator's muscle strength was augmented and it would be easier to drive the robot. In mode *c*, λ was set to -0.5 (resistive mode is simulated), indicating the operator's active effort was weakened and the control task was more challenging.

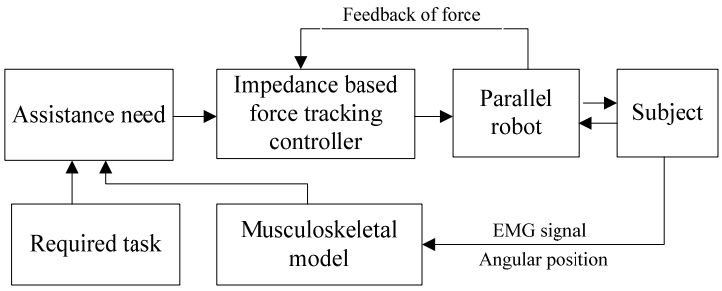

Fig.7 Framework for the model based AAN control scheme

However, it can be seen that in the first group, the robot was controlled to provide the predefined assistance, since λ was fixed during the experiment. In this situation, the control interface did not take into account the subject's changing needs in real time. To evaluate if the musculoskeletal model can be used to automatically adjust the robotic assistance, in the second group a model based AAN control scheme was developed. Since the subject's active effort can be estimated by the musculoskeletal model, once the required task was determined, the assistance need can be obtained. To this end, the framework for the model based AAN control scheme can been given as shown in Fig.7. An impedance based force tracking controller was used to guide the robot to provide the assistance that governed by the musculoskeletal model and task. For convenience, the required task was set to a constant.

4.2. Experimental Results

In this section, the experimental results of robot control are presented. The kinematic performances of the robot in the first group are presented in Fig.8. The adjustment process of robotic assistance in the second group is presented in Fig.9. As stated before, in the free mode the robot was controlled to synchronously track the subject's trajectory. The tracking performance is acceptable as shown in Fig.8 (a), where close agreement in shape and magnitude were observed. The average RMSE value was 4.11° , indicating the proposed model based control interface is capable of detecting the operator's motion intention in real time. The main reason for the tracking error is that the EMG signals are sensitive to many uncertain factors such as skin noise and electrode placement.

The results of assistive mode illustrated in Fig.8 (b) clearly show that the ROM of robot was larger than the subject's ROM. In contrast, the robot's ROM reduced distinctly in resistive mode, although the ROM of subject remained almost the same. It demonstrates that in assistive mode the subject can drive the robot to reach a certain ROM with less effort compared with that in resistive mode where the subject's contribution was weakened, and it required more voluntary efforts to complete the task. Therefore, different control modes can be achieved by adjusting the parameter λ to cater for the requirements of different patients.

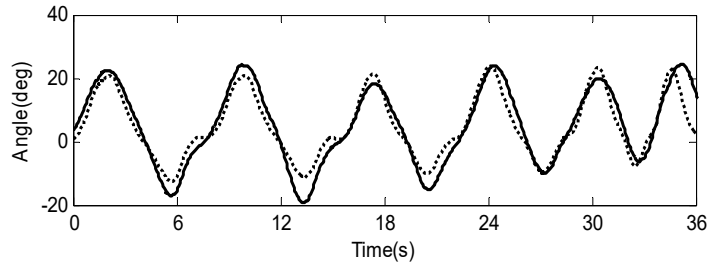

(a) Results of free mode

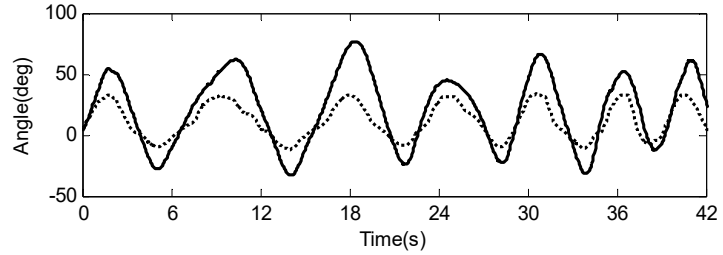

(b) Results of assistive mode

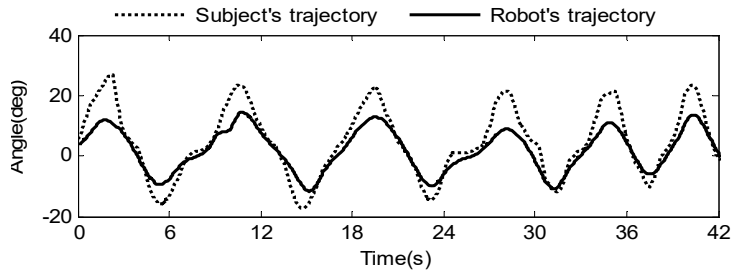

(c) Results of resistive mode

Fig.8. Comparison of kinematic performance in the first group of experiments. The dashed lines are the subject's movement trajectories and the solid lines represent the robot's movement trajectories.

The results of the second group illustrated in Fig.9 clearly show that during the experiment, both the subject's active effort and the actual assistance he received were changed over time. It demonstrated that the subject had actively participated into the experiment and the robotic assistance was adjustable rather than inflexible. One can note that the increase of active effort applied by the subject would lead to the instant decrease of robotic assistance and vice versa. It demonstrated that musculoskeletal model based ANN controller was capable of adjusting the robotic assistance in real time according to the subject's voluntary effort. In this situation, the control method encourages the subject's voluntary participation in rehabilitation training which may induce brain

plasticity and motor recovery. Moreover, during the rehabilitation training subject's active effort may gradually decrease, which can be caused by the muscle fatigue. Hence, in order to enhance the rehabilitation outcome, it is important for robot to learn the subject's physical ability in real time and to provide assistance accordingly.

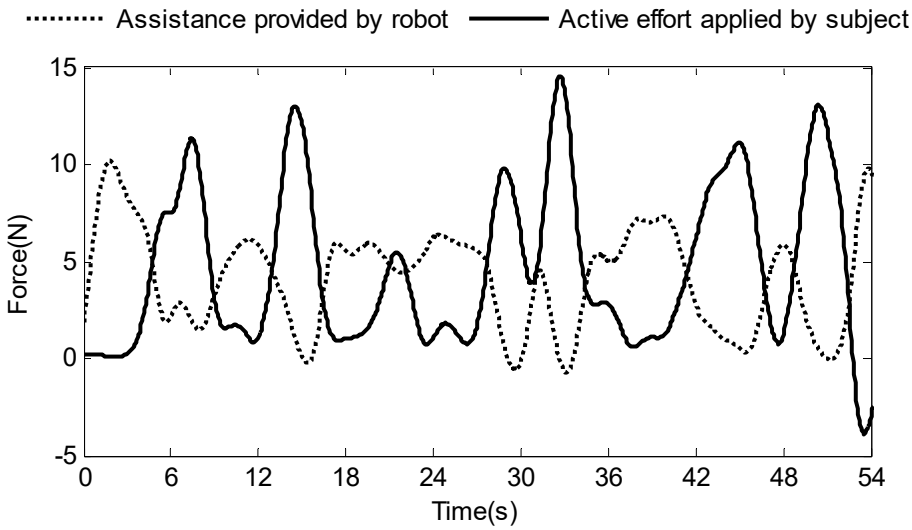

Fig.9. Adjustment process of robotic assistance in the second group of experiments. The dashed line represents the assistance provided by the robot and the solid line indicates the active effort applied by the subject.

5. Discussion

5.1. Benefits

The proposed subject-specific EMG-driven musculoskeletal model and model based control approach have several benefits over existing models and methods. The relationship between EMG signals and joint torque was modeled from the perspective of biomechanics. As a result, the obtained model is capable of accurately identifying the subject's joint torque and monitoring his/her muscle status, as shown in Fig.4 and Fig.5. Unlike the sample training based torque estimation method,[32] musculoskeletal model based method is more meaningful and accurate, since most of the muscles in relation to movement are taken into account and are physiologically modeled.

A practical method to study the subject-specific musculoskeletal geometry is included in the whole model. As stated before, generic musculoskeletal geometry may not suitable for specific individuals. In this paper, subject-specific musculoskeletal geometry was estimated based on the measured skeletal morphologic parameters. Since muscles are attached to skeletons, it is reasonable to estimate the muscle paths according to morphologic parameters.[33, 34] This method has been proved to be feasible in identification process, where the results clearly show that the estimated torque could successfully track

the reference torque with an acceptable accuracy. Furthermore, in order to test whether the proposed model with the subject-specific musculoskeletal geometry can improve the prediction accuracy, the model was re-calibrated with a generic musculoskeletal geometry. The prediction performance became worse as shown in Table 2, where the R^2 values reduced from 0.934 to 0.900 and the normalized RMSE values increased from 11.58% to 15.57%. This finding shows the importance of acquiring more accurate musculoskeletal geometry.

The ability of the proposed musculoskeletal model to predict joint moment is better compared to existing models as summarized in Table 4. Shao et al. had developed a musculoskeletal model to estimate ankle joint moment with the normalized RMSE and average R^2 of 12.2% and 0.92, respectively.[35] Lloyd and Besier's model was able to predict knee joint moment for various dynamic tasks, such as running and cutting, and the average R^2 was 0.91.[20] However, both of the two models employed a generic geometry model to analyze moment arm. In this paper, better results were obtained by using a subject-specific musculoskeletal geometry model, where the average R^2 was 0.934 ± 0.013 and the normalized RMSE was $11.58\% \pm 1.44\%$. Ma et al. used only two channels of EMG signals (one flexor and one extensor) to predict the knee joint moment.[36] Although their model was greatly simplified, the accuracy was limited (R^2 <0.85). Moreover, Tsai et al. used the directly measured data obtained by MRI to create specific geometry model and their results suggested that the moment arm estimated by imaging techniques can improve the joint moment prediction performance.[23] However, image processing may be time-consuming, which is not suitable for on-line applications such as rehabilitation robot control.

Table 4 Comparison of existing EMG-driven musculoskeletal models and the proposed model (*, Unknown)

Literatures	Joint modeled	Number of subjects	Average R^2	Normalized RMSE
21	Ankle	4	0.92	12.2%
20	Knee	6	0.91	*
33	Knee	1	<0.85	17%
Current study	Knee	6	0.934	11.58%

This model-based interface makes the intuitive, continuous and accurate robot control possible. Recently, many EMG-based control methods have been proposed, such as EMG proportional control and EMG pattern recognition based control.[37] Nonetheless, EMG proportional control can not accurately detect the operator's motion intention and pattern

recognition based control breaks the continuous movement into discrete and limited patterns. The kinematic performance of robot in Fig.8 (a) demonstrates that the proposed model based control is capable of providing continuous, intuitive and accurate (RMES = 4.11 °) motor commands rather than discrete motion patterns or rough motion information. Since the natural movements of human are continuous, the patient may benefit much more if the rehabilitation robot can be controlled in this way. Furthermore, the model-based interface is adjustable to operator's physical capability to realize different control mode. Generally, patients with different recovery conditions need to be treated with different training modes. As the operator's joint torque can be estimated by the musculoskeletal model, different control modes were achieved by adjusting the level of assistance as shown in Fig.8. It may be argued that the different control modes were simply achieved by adjusting the proportional parameter, which is similar to EMG proportional control method. However, as shown in Fig.4, muscle activation pattern varies form people to people and EMG values of a certain muscle can not accurately reflect the subject's actual joint torque. Hence, adjusting the control modes according to EMG value is inappropriate and it is more reasonable to adjust the robotic assistance at the level of muscular torque.

Model-based interface has the potential to automatically adjust the robotic assistance in real time according to the patient's voluntary effort. In the field of robot-assisted rehabilitation, it is assumed that once the patient has regained some strength, the robotic assistance should decrease since relying too much on the robotic devices may have negative consequences for brain plasticity and motor recovery. AAN control method is a promising solution to this problem, which aims to minimize the robotic assistance required to help the operator complete the task. The main challenge to implement the AAN control strategy on robotics is how to determine the true assistance needs of the operator in real time. A well-developed method is to adaptively adjust the robotic assistance according to the operator's performance.[38-42] In these literatures, the increase of performance error will lead to the increase of robotic assistance and vice versa. However, for this performance-based AAN method, the robotic assistance was adjusted empirically. Moreover, how to appropriately select the criterion to evaluate the performance has not been settled yet. Since the subject's active effort can be estimated by the musculoskeletal model, for the given tasks the true assistance needs can be obtained easily, namely, the difference between the required and active force. As shown in Fig.9, the model based AAN controller is capable of adjusting the robotic assistance in real time according to the subject's active effort rather than providing inflexible assistance.

5.2. Limitations

Although only knee joint was taken into account, the related musculoskeletal model is very complex and many parameters need to be identified to make them specific to subjects. However, the authors did not have a strong knowledge of the biomechanical theory before, but we will absolutely learn the related knowledge in our future works. Moreover, the identification process, comprised of online data acquisition and offline

optimization, is time-consuming. Therefore, some assumptions were made in this paper to simplify the model. It is assumed that the same normalized active force-length, force-velocity, passive force-length and tendon-force are suitable for all muscles. However, physiologically different muscles may have different activation dynamics and contraction dynamics. As for the musculoskeletal geometry, skeletal morphologic parameters measured from the subject were used to estimate the origin and insertion coordinates of muscles, which was proved to be feasible but may not anatomically accurate.

Since the model is driven by EMG signals, the proposed human-robot interface has some drawbacks like many EMG-based control methods.[43] The EMG signals are sensitive to many uncertain factors such as skin noise and electrode placement. Hence, the differences between the EMG signals obtained during the same motions are inevitable. Moreover, there are biarticular muscles involved in the musculoskeletal model. The biarticular muscles refer to muscles connected with motions of two joints (e.g., The RF contribute to motions both of knee and hip joint). As a result, the EMG signals obtained from the RF were affected not only by motions of knee but also by motions of hip.

6. Conclusion and Future Work

In this paper, a subject-specific musculoskeletal model in relation to knee joint is presented to estimated the subject's joint torque in real-time and to make contribution in robot-assisted rehabilitation. Considering that the operator's physical capability has large person-to-person variation, the model parameters were identified through an off-line optimization procedure. Results of validation experiments demonstrated the model was able to predict knee joint torque with high R^2 value and small normalized RMSE. Experimental results also showed the importance of acquiring more accurate musculoskeletal geometry. Moreover, the experiments with a lower-limb rehabilitation robot showed that the model can be used to realize different control modes. Future work should be invested in conducting experiments on patients to test whether the proposed strategy can actually enhance the rehabilitation outcomes. Since only knee joint was involved in the musculoskeletal model, future investigation should take into account the hip and ankle to develop control interface that can provide assistance in gait training.

Acknowledgments

This research is funded and supported by the National Natural Science Foundation of China (Grant No.51475342) and the Fundamental Research Funds for the Central Universities (Grant No.2015-zy-092).

References

1. L. Marchal-Crespo and D. J. Reinkensmeyer, Review of control strategies for robotic movement training after neurologic injury, *Journal of Neuroengineering and Rehabilitation* 6(2009).
2. W. Meng, Liu, Q., Zhou, Z., Ai, Q., Sheng, B., & Xie, S. S., Recent development of mechanisms and control strategies for robot-assisted lower limb rehabilitation, *Mechatronics* (2015).
3. S. Hussain, S. Q. Xie, and G. Liu, Robot assisted treadmill training: Mechanisms and training strategies, *Medical Engineering & Physics* 33(5) (2011) 527-533.
4. T. Lenzi, S. M. M. De Rossi, N. Vitiello, and M. C. Carrozza, Intention-Based EMG Control for Powered Exoskeletons, *Ieee Transactions on Biomedical Engineering* 59(8) (2012) 2180-2190.
5. Q. S. Ai, Q. Liu, T. T. Yuan, and Y. Lu, Gestures recognition based on wavelet and LLE, *Australasian Physical & Engineering Sciences in Medicine* 36(2) (2013) 167-176.
6. Y. F. Fang, H. H. Liu, G. F. Li, and X. Y. Zhu, A Multichannel Surface EMG System for Hand Motion Recognition, *International Journal of Humanoid Robotics* 12(2) (2015).
7. K. Kiguchi, Active exoskeletons for upper-limb motion assist, *International Journal of Humanoid Robotics* 4(3) (2007) 607-624.
8. W. Meng, Q. Liu, Z. D. Zhou, and Q. S. Ai, Active interaction control applied to a lower limb rehabilitation robot by using EMG recognition and impedance model, *Industrial Robot-an International Journal* 41(5) (2014) 465-479.
9. N. Jiang, K. B. Englehart, and P. A. Parker, Extracting Simultaneous and Proportional Neural Control Information for Multiple-DOF Prostheses From the Surface Electromyographic Signal, *Ieee Transactions on Biomedical Engineering* 56(4) (2009) 1070-1080.
10. Q. J. Song, Y. Yu, Y. J. Ge, Z. Gao, H. H. Shen, and X. H. Deng, A real-time emg-driven arm wrestling robot considering motion characteristics of human upper limbs, *International Journal of Humanoid Robotics* 4(4) (2007) 645-670.
11. K. Kiguchi, T. Tanaka, and T. Fukuda, Neuro-fuzzy control of a robotic exoskeleton with EMG signals, *Ieee Transactions on Fuzzy Systems* 12(4) (2004) 481-490.
12. A. Erdemir, S. McLean, W. Herzog, and A. J. van den Bogert, Model-based estimation of muscle forces exerted during movements, *Clinical Biomechanics* 22(2) (2007) 131-154.
13. M. G. Carmichael and D. Liu, Towards using musculoskeletal models for intelligent control of physically assistive robots, *Conference proceedings : ... Annual International Conference of the IEEE Engineering in Medicine and Biology Society. IEEE Engineering in Medicine and Biology Society. Annual Conference* 2011((2011) 8162-5.
14. M. G. Carmichael and D. K. Liu, Estimating Physical Assistance Need Using a Musculoskeletal Model, *Ieee Transactions on Biomedical Engineering* 60(7) (2013) 1912-1919.
15. W. Hassani, S. Mohammed, H. Rifai, and Y. Amirat, Powered orthosis for lower limb movements assistance and rehabilitation, *Control Engineering Practice* 26((2014) 245-253.
16. J. W. L. Pau, S. S. Q. Xie, and A. J. Pullan, Neuromuscular Interfacing: Establishing an EMG-Driven Model for the Human Elbow Joint, *Ieee Transactions on Biomedical Engineering* 59(9) (2012) 2586-2593.

17. T. S. Buchanan, D. G. Lloyd, K. Manal, and T. F. Besier, Neuromusculoskeletal modeling: Estimation of muscle forces and joint moments and movements from measurements of neural command, *Journal of Applied Biomechanics* 20(4) (2004) 367-395.
18. T. S. Buchanan, D. G. Lloyd, K. Manal, and T. F. Besier, Estimation of muscle forces and joint moments using a forward-inverse dynamics model, *Medicine and Science in Sports and Exercise* 37(11) (2005) 1911-1916.
19. S. L. Delp, F. C. Anderson, A. S. Arnold, P. Loan, A. Habib, C. T. John, E. Guendelman, and D. G. Thelen, OpenSim: open-source software to create and analyze dynamic Simulations of movement, *Ieee Transactions on Biomedical Engineering* 54(11) (2007) 1940-1950.
20. D. G. Lloyd and T. F. Besier, An EMG-driven musculoskeletal model to estimate muscle forces and knee joint moments in vivo, *Journal of Biomechanics* 36(6) (2003) 765-776.
21. D. G. Thelen, Adjustment of muscle mechanics model parameters to simulate dynamic contractions in older adults, *Journal of Biomechanical Engineering-Transactions of the Asme* 125(1) (2003) 70-77.
22. F. E. Zajac, Muscle and tendon: properties, models, scaling, and application to biomechanics and motor control, *Critical reviews in biomedical engineering* 17(4) (1989) 359-411.
23. L.-C. Tsai, P. M. Colletti, and C. M. Powers, Magnetic Resonance Imaging-Measured Muscle Parameters Improved Knee Moment Prediction of an EMG-Driven Model, *Medicine and Science in Sports and Exercise* 44(2) (2012) 305-312.
24. D. Shan, Brief introduction of research on model parameters of human lower body muscle function, *Journal of Shanghai physical education Institute* 28(4) (2004) 63-68.
25. F. De Groote, A. Van Campen, I. Junkers, and J. De Schutter, Sensitivity of dynamic simulations of gait and dynamometer experiments to hill muscle model parameters of knee flexors and extensors, *Journal of Biomechanics* 43(10) (2010) 1876-1883.
26. C. Redl, M. Gfoehler, and M. G. Pandy, Sensitivity of muscle force estimates to variations in muscle-tendon properties, *Human Movement Science* 26(2) (2007) 306-319.
27. M. L. Audu and D. T. Davy, The influence of muscle model complexity in musculoskeletal motion modeling, *Journal of biomechanical engineering* 107(2) (1985) 147-57.
28. A. B. Ajiboye and R. F. Weir, Muscle synergies as a predictive framework for the EMG patterns of new hand postures, *Journal of Neural Engineering* 6(3) (2009).
29. S. L. Delp, J. P. Loan, M. G. Hoy, F. E. Zajac, E. L. Topp, and J. M. Rosen, An interactive graphics-based model of the lower extremity to study orthopaedic surgical procedures, *IEEE transactions on bio-medical engineering* 37(8) (1990) 757-67.
30. Z. Zhou, W. Meng, Q. S. Ai, Q. Liu, and X. Wu, Practical Velocity Tracking Control of a Parallel Robot Based on Fuzzy Adaptive Algorithm, *Advances in Mechanical Engineering* (2013).
31. Q. Liu, D. Liu, W. Meng, Z. D. Zhou, and Q. S. Ai, Fuzzy Sliding Mode Control of a Multi-DOF Parallel Robot in Rehabilitation Environment, *International Journal of Humanoid Robotics* 11(1) (2014).

32. R. Song and K. Y. Tong, Using recurrent artificial neural network model to estimate voluntary elbow torque in dynamic situations, *Medical & Biological Engineering & Computing* 43(4) (2005) 473-480.
33. M. D. K. Horsman, H. F. J. M. Koopman, F. C. T. van der Helm, L. P. Prose, and H. E. J. Veeger, Morphological muscle and joint parameters for musculoskeletal modelling of the lower extremity, *Clinical Biomechanics* 22(2) (2007) 239-247.
34. T. M. Kepple, H. J. Sommer, 3rd, K. Lohmann Siegel, and S. J. Stanhope, A three-dimensional musculoskeletal database for the lower extremities, *Journal of biomechanics* 31(1) (1998) 77-80.
35. Q. Shao, D. N. Bassett, K. Manal, and T. S. Buchanan, An EMG-driven model to estimate muscle forces and joint moments in stroke patients, *Computers in Biology and Medicine* 39(12) (2009) 1083-1088.
36. Y. Ma, S. Q. Xie, and Y. Zhang, A Patient-Specific EMG-Driven Musculoskeletal Model for Improving the Effectiveness of Robotic Neurorehabilitation, *Lecture Notes in Computer Science (including subseries Lecture Notes in Artificial Intelligence and Lecture Notes in Bioinformatics)* 8917((2014) 390-401.
37. R. Song, K.-y. Tong, X. Hu, and L. Li, Assistive control system using continuous myoelectric signal in robot-aided arm training for patients after stroke, *Ieee Transactions on Neural Systems and Rehabilitation Engineering* 16(4) (2008) 371-379.
38. H. I. Krebs, J. J. Palazzolo, L. Dipietro, B. T. Volpe, and N. Hogan, Rehabilitation robotics: Performance-based progressive robot-assisted therapy, *Autonomous Robots* 15(1) (2003) 7-20.
39. R. Riener, L. Lunenburger, S. Jezernik, M. Anderschitz, G. Colombo, and V. Dietz, Patient-cooperative strategies for robot-aided treadmill training: First experimental results, *Ieee Transactions on Neural Systems and Rehabilitation Engineering* 13(3) (2005) 380-394.
40. A. Duschau-Wicke, J. von Zitzewitz, A. Caprez, L. Luenenburger, and R. Riener, Path Control: A Method for Patient-Cooperative Robot-Aided Gait Rehabilitation, *Ieee Transactions on Neural Systems and Rehabilitation Engineering* 18(1) (2010) 38-48.
41. L. L. Cai, A. J. Fong, C. K. Otoshi, Y. Liang, J. W. Burdick, R. R. Roy, and V. R. Edgerton, Implications of assist-as-needed robotic step training after a complete spinal cord injury on intrinsic strategies of motor learning, *Journal of Neuroscience* 26(41) (2006) 10564-10568.
42. U. Keller, G. Rauter, and R. Riener, Assist-as-needed path control for the PASCAL rehabilitation robot, in *Rehabilitation Robotics (ICORR), 2013 IEEE International Conference on*, 2013(2013) 1-7.
43. K. Kiguchi and Y. Hayashi, An EMG-Based Control for an Upper-Limb Power-Assist Exoskeleton Robot, *Ieee Transactions on Systems Man and Cybernetics Part B-Cybernetics* 42(4) (2012) 1064-1071.

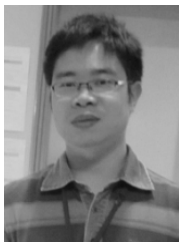

Qingsong Ai received his M.S. and Ph.D. degrees from the Wuhan University of Technology, China, in 2006 and 2008, respectively. From 2006 to 2007, he was a visiting researcher at the Faculty of Engineering, University of Auckland, New Zealand, and worked on the project of medical robots. He was the Professor at the Wuhan University of Technology. Now, he is senior editor of Cogent Engineering. Qingsong Ai is the author of over 35 technical publications, proceedings, and editorials. In recent years, he has directed more than 10 research projects. His research interests include signal processing, rehabilitation robots and advanced manufacturing technology.

Bo Ding received his B. Eng. degree from Wuhan University of Technology, China, in 2013. From 2013 to 2016, he is pursuing a M.S. degree in Wuhan University of Technology. He has participated in two research projects in areas of rehabilitation robots and interaction control. His research interests include robot-assisted rehabilitation, EMG-based interactive control and musculoskeletal model based control.

Quan Liu received her Ph.D. degree from the Wuhan University of Technology, China, in 2003. Now, she is the professor at the Wuhan University of Technology. She is the Council Member of Chinese Association of Electromagnetic Compatibility and the Hubei Institute of Electronics, and she is also an IEEE member. During the recent five years, Quan Liu has authored or co-authored over 60 technical publications, proceedings, editorials and books. She has also directed more than 20 research projects. Her research interests include signal processing, robot hardware and electronics, embedded systems and applications.

Wei Meng received his B. Eng. degree and the M. Eng. degree from Wuhan University of Technology, China, in 2010 and 2013, respectively. From 2012 to 2016, he is pursuing his study as a joint PhD. student in Wuhan University of Technology and The University of Auckland, New Zealand. He has directed two research projects and participated in over five research projects in areas of rehabilitation robots, bio-signals processing and interaction control. Wei Meng is the author of over 10 academic journal and conference papers. His research interests include the robot-assisted rehabilitation, human-robot interaction and adaptive impedance control.